

Investigating possibilities for synthesis of novel sorbents and catalyst carriers based on ceramics with controlled open porosity

Vesna D. Nikolić¹, Jovana M. Đokić², Željko J. Kamberović³, Aleksandar D. Marinković³, Sanja O. Jevtić³ and Zoran M. Anđić²

¹Innovation Centre of the Faculty of Technology and Metallurgy, Belgrade, Serbia

²Innovation Centre of the Faculty of Chemistry, Belgrade, Serbia

³University of Belgrade, Faculty of Technology and Metallurgy, Belgrade, Serbia

Abstract

The aim of this study was to investigate a possibility of synthesis of porous ceramics with controlled open porosity, which could be used as sorbents and catalyst supports. Two organic additives were used to obtain open porosity: polystyrene beads and cellulose fibers, which are mixed with kaolin clay powder and the appropriate water content. Samples were sintered at 1050 °C for 1 h. Characterization of the obtained products included X-ray powder diffraction analysis (XRPD), Fourier-transform infrared spectroscopy (FTIR), scanning electron microscopy (SEM), thermogravimetric analysis (TGA) and elemental CHNS analysis. In addition, porosity was examined by quantification of visual information. The specific surface areas were determined by the Brunauer–Emmett–Teller (BET) method. Also, density and compressive strength of the obtained samples were assessed. It was determined that by sintering, the organic component completely leaves the system. For samples prepared with polystyrene beads and with cellulose fibers, satisfactory mechanical properties were obtained: compressive strengths were 1.42 and 1.56 MPa, respectively. It was noted that significantly higher open porosity was obtained by using polystyrene beads as a sacrificial template (porosity of ~56 %) instead of cellulose fibers (porosity of ~6 %).

Keywords: porous sintered clay; kaolin; polystyrene; cellulose fibers.

Available on-line at the Journal web address: <http://www.ache.org.rs/HI/>

ORIGINAL SCIENTIFIC PAPER

UDC: 543.544-414.5:666.3.017:
620.192.47:

Hem. Ind. **76** (2) 87-95 (2022)

1. INTRODUCTION

High levels of heavy metals, metalloids, drugs, and other pollutants present in the environment may represent long-term risks to human health and ecosystems, and therefore they have to be lowered to at least maximum allowable concentrations that the World Health Organization has recommended [1]. Amongst many methods for removal of pollutants from water, adsorption technology is mostly applied due to the highest efficiency [2-4].

Porous ceramics are widely used in adsorption, but also in heterogeneous catalysis to support catalytically active substances for waste gas treatment due to high porosity and permeability to liquids, as well as high thermal stability and low density of these materials [5-13]. There are numerous methods for the synthesis of either porous solid shapes or fine particles based on ceramics such as polymer replication [10,14], modified sol-gel method [12,15], sintering of green bodies prepared from starting ceramic powders [14,16], external gelatinization [17], etc. For example, a suspension of polymer particles in AlF_3 was sintered to burn the polymer template and form reactive aluminum foam filters for the purification of molten aluminum [11]. Also, reticulated ceramic foams were prepared by dipping a polymer foam into ceramic slurry, controlled drying (60 °C for 72 h then 100 °C for 1 h) followed by sintering at 1250 °C for 2 h resulting in foams of various shapes and broad porosity range [14]. Mesoporous γ -alumina adsorbents for heavy metal removal were synthesized by a method based on modified sol-gel, using polymethyl methacrylate microspheres as templates for obtaining mesopores, while the alumina precursor was aqueous solution of $Al_2Cl(OH)_5 \times 2.5H_2O$. After

Corresponding authors: Vesna D. Nikolić, Innovation Centre of the Faculty of Technology and Metallurgy, Belgrade, Serbia

E-mail: vnikolic@tmf.bg.ac.rs

Paper received: 9 August 2021; Paper accepted: 21 March 2022; Paper published: 21 April 2022.

<https://doi.org/10.2298/HEMIND210809005N>



mixing, compressing, drying (48 h at 40 °C) and sintering at 800 °C for 5 h, highly efficient adsorbents for Pb²⁺, Ni²⁺ and Cd²⁺ with highly ordered porosity were obtained [12]. Similarly, macroporous γ -alumina spheres were produced by an external gelatinization, sol-gel based process for potential applications as adsorbents [17]. Activated γ -alumina powder was mixed with alumina sol, medium density fibreboard (MDF) powder and chemical precipitation media to enable the sol-gel transformation. The obtained gel spheres were aged, washed, dried and calcined at temperatures from 600 to 1250 °C. The developed production method is efficient in the conservation of microporosity of the spheres, shown to be good adsorbents for Cd²⁺, Cu²⁺ and Zn²⁺ [17]. Porous alumina was also obtained from ceramic powders without using a polymer template by mixing corundum powders with aluminum hydroxide, which decomposed during the thermal treatment, and sintering at 1000 °C for 30 min. It was concluded that the fracture strength and fracture toughness were increased compared to ceramic prepared with only corundum when 90 wt.% of Al(OH)₃ was mixed with corundum powder, and at the same time, highest porosity of some samples reached 62 % [16]. By described polymer foam replication or sacrificial template (polymethyl methacrylate microspheres) replication methods, desired shape and porosity of ceramics are obtained by burnout of the templates during sintering [12,18]. In addition, controlled open porosity in ceramic foams can be formed by gas bubbles, obtained by the use of foaming agents during ceramic preparation [19]. Previous studies have shown that it is possible to use NaOH as an effective foaming agent for the preparation of glass or glass-ceramic foams. Starting powders of soda lime glass were mixed with a solution of NaOH (10 wt.%) and sintered at about 750 °C in order to obtain a porosity of up to 92 % [20-23].

The aim of this study was to examine the possibility of synthesis of ceramic sorbents and / or catalyst carriers with controlled open porosity, which will provide a high degree of sorption and homogeneous precipitation of catalytically active substances, *i.e.* high catalytic activity. In order to obtain porous ceramics with a hierarchically arranged controlled open porosity, polystyrene beads and cellulose fibers were used for the first time as a sacrificial template mixed with kaolin clay powder and appropriate water content.

2. EXPERIMENTAL

2. 1. Materials and methods

In order to synthesize porous ceramic samples, the following materials were used: kaolin clay powder (99 %, Zorka Alas Kamen, Serbia), cellulose fibers (Đurašković Aleksej Ltd., Serbia), crosslinked polystyrene beads with phosphate groups (Lewatit® VP OC 1026, Lanxess, Germany) and demineralized water.

Kaolin clay powder had particle size of 99 % under 43 μ m, and the following chemical composition: SiO₂ 69.20 wt.%, Al₂O₃ 18.90 wt.%, Fe₂O₃ 1.40 wt.%, TiO₂ 0.83 wt.%, CaO 0.42 wt.%, MgO 0.46 wt.%, Na₂O 0.10 wt.% and K₂O 2.89 wt.% as provided by the producer (Zorka Alas Kamen, Serbia). Polystyrene beads had particle diameter in the range from 0.31 to 1.65 mm.

Samples with polystyrene beads (G-PS-G) were obtained by mixing beads with dry powder of kaolin clay. The content of the beads was 27 wt.% (of total weight), which corresponds to about 70 vol.% of the dry mixture. After 15 min of mixing dry components, 40 wt.% of water was slowly added, and the mixture was stirred for another 15 min by using an IKA Eurostar 20 mechanical mixer (IKA-Werke GmbH & Co., Germany) at 250 rpm until thick paste was obtained. The content of water was previously determined experimentally and that is the minimal water content needed to obtain the paste that can be stirred by a mechanical mixer at 250 rpm. The paste was then manually pressed into cylinders in gypsum molds. The obtained green samples, G-PS-G, were dried in air atmosphere for 48 h at room temperature. Slow drying was carried out in order to prevent cracking and to distribute humidity evenly in the volume of samples.

The samples with cellulose fibers as a sacrificial template (G-CV-G) were prepared under the same conditions as the samples with polystyrene. To allow mixing by a mechanical mixer at the same speed as in the G-PS-G sample, about the amount of water added was about four-fold higher. The water content was previously determined experimentally as the minimal amount that enables stirring of the paste by mechanical mixer at the specified speed. The cellulose content in the paste was 30 wt.%, and in the dry mixture it was approximately 70 %.

Green samples (G-PS-G and G-CV-G) were then removed from molds and sintered at 1050 °C for 1 h to obtain the final product (heating rate of 5 °C min⁻¹). The obtain samples after sintering were denoted as G-PS-S (sample with polystyrene) and G-CV-S (sample with cellulose fibers). During each synthesis, five green samples were made and subsequently sintered.

2. 2. Characterization

Crystallographic structure investigation (X-ray powder diffraction, XRPD) of green and sintered samples was performed by using the Roentgen diffractometer ("Philips", model PW-1710, Philips, Netherlands) with a curved graphite monochromator and a scintillation counter. Intensities of the diffracted CuK_α Roentgen radiation ($\lambda = 1.54178 \cdot 10^{-10}$ m) were measured at room temperature at 0.02° intervals of 2θ , in the range 5 – 80°. The presence of the organic sacrificial templates in green and sintered samples was determined by Fourier-transform infrared spectroscopy (FTIR) using FTIR BOMEM MB series (Hartmann & Braun, country), in the range 4000-500 cm⁻¹ with a resolution of 4 cm⁻¹ in the form of KBr pellets. Thermogravimetric analysis (TGA) was performed by using a SDT Q-600 TA Instruments device (producer, country). The samples were heated in an alumina sample pan from room temperature to 700 °C at a heating rate of 10 °C min⁻¹ under nitrogen flow rate of 100 cm³ min⁻¹. Amounts of carbon in the samples after sintering were determined by a Vario EL cube - Elementar CHNS analyzer (producer, country). The specific surface areas were determined by the Brunauer–Emmett–Teller (BET) method, using an automated gas adsorption analyzer Micrometrics ASAP 2020 (producer, country). The morphology of the sintered samples was analyzed by using a Field Emission Scanning Electron Microscope (FESEM, TESCAN MIRA 3, producer, country)). Open porosity was examined at SEM images of sintered samples by using KVI software for quantification of visual information. Density values of the sintered samples were determined from the ratio of mass and volume. Afterwards, compressive strength of disc shaped specimens with diameter of 30 mm was determined by using a servo hydraulic machine Shimadzu UH - F1000kNI (producer, country) at the piston speed of 2 mm min⁻¹. All analyses were performed by using minimum 5 replicate measurements.

3. RESULTS

Diffractograms of green (G-PS-G and G-CV-G) and sintered (G-PS-S and G-CV-S) samples are presented in Figure 1. Distinct peaks of kaolin, quartz and polystyrene or cellulose are observed in non-sintered samples. After sintering, kaolin peaks intensity decreases, the organic component completely disappears, while a phase which can be attributed to aluminum-silicon spinel appears.

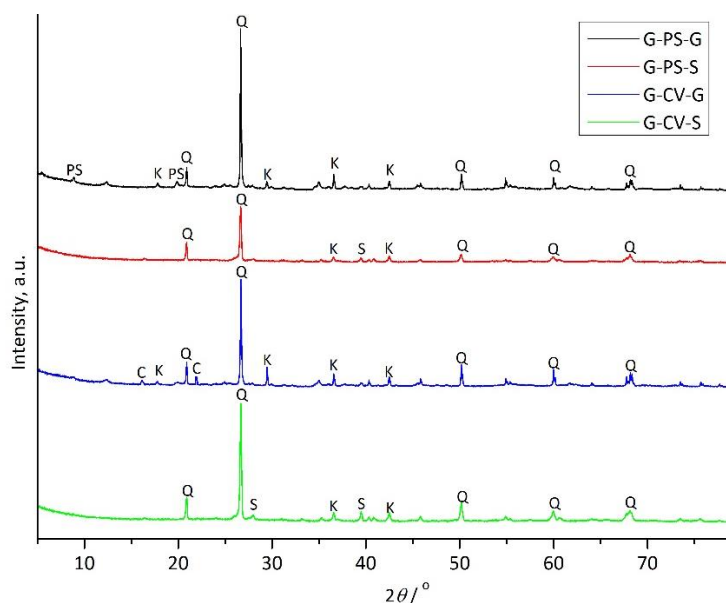


Figure 1. XRD spectra of green and sintered samples (K – kaolinite, Q – quartz, S - aluminum-silicon spinel, PS – polystyrene, C – cellulose)



FTIR spectra of the green and sintered samples are presented in Figures 2 and 3.

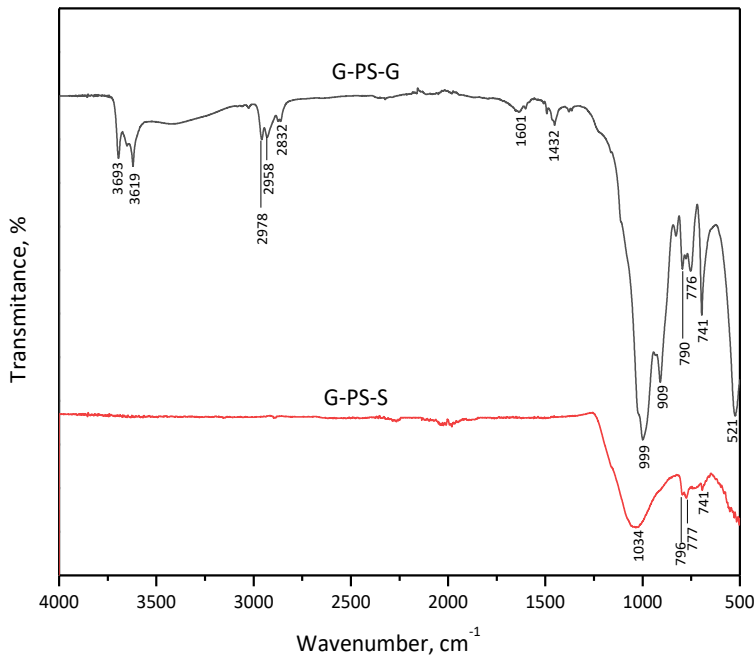


Figure 2. FTIR spectra of green (G-PS-G) and sintered (G-PS-S) samples prepared with polystyrene beads

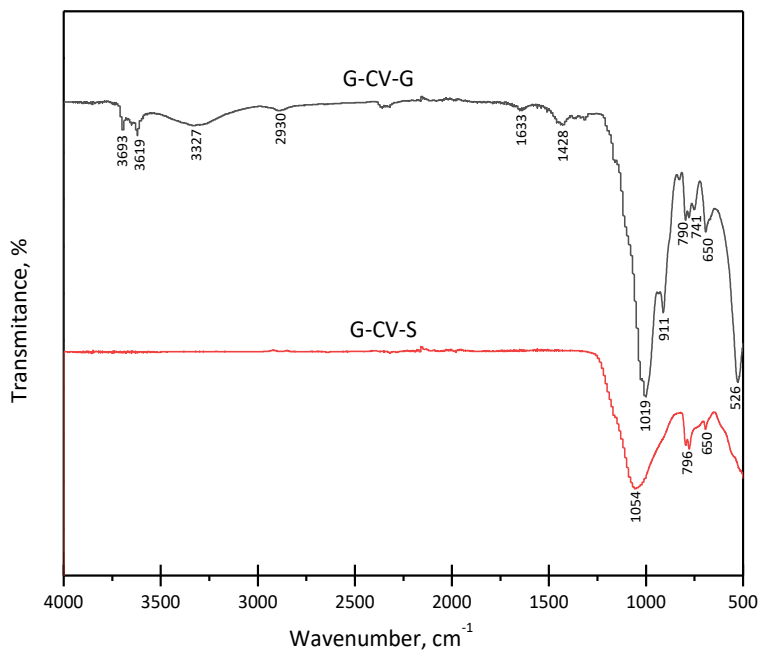


Figure 3. FTIR spectra of green (G-CV-G) and sintered (G-CV-S) samples prepared with cellulose fibers

The results of the TGA analysis are shown in Figure 4. The total weight loss in the sample G-PS-S was 0.44 %, while in the sample G-CV-S it was 0.31 %, which correspond to residues of organic components remaining after sintering.

The CHNS analysis has shown carbon contents of 0.13 and 0.1 wt.% in G-PS-S and G-CV-S samples, respectively.

The specific surface area of G-PS-S and G-CV-S samples was determined by the BET analysis yielding 0.33 m² g⁻¹ for G-PS-S and less than 0.2 m² g⁻¹ for G-CV-S.

SEM images of sintered porous ceramic samples are presented in Figure 5.

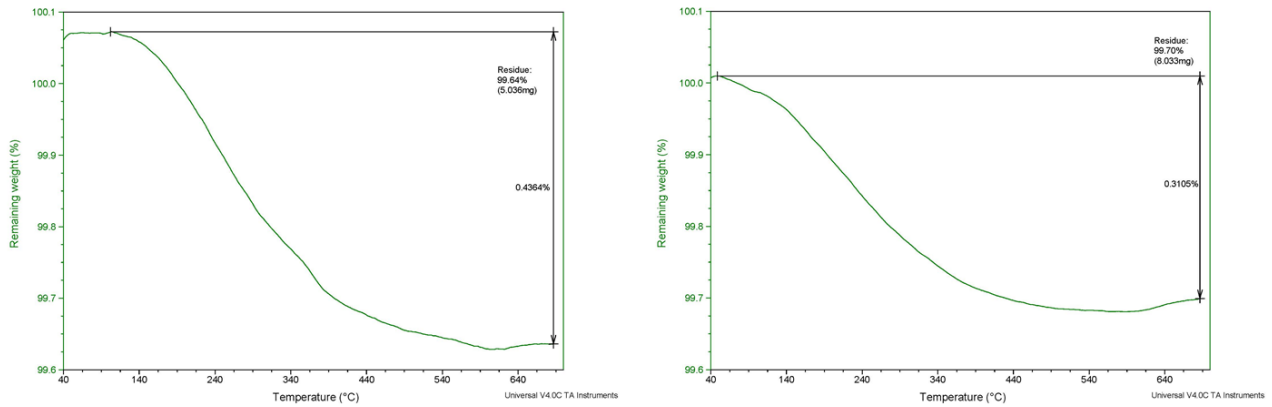


Figure 4. Thermograms of sintered G-PS-S and G-CV-S samples

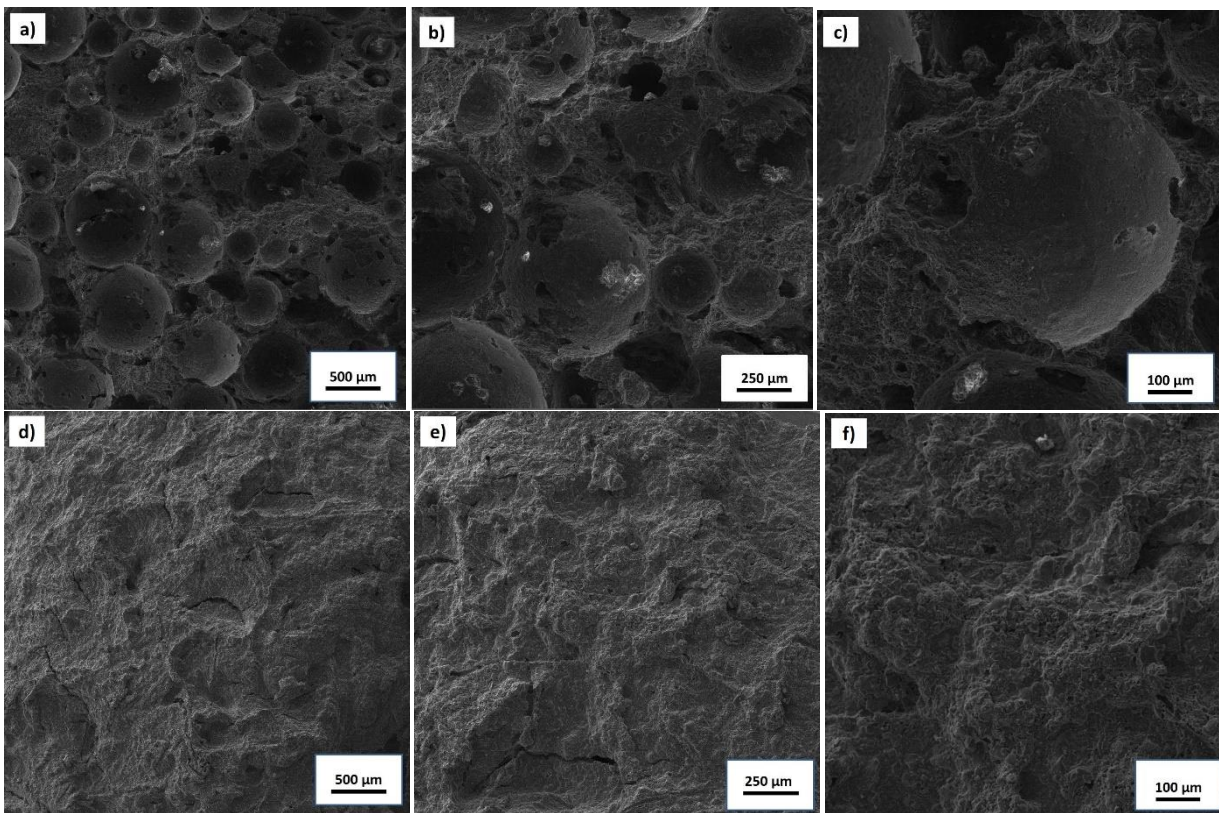


Figure 5. SEM images of sintered porous ceramics: G-PS-S (a-c) and G-CV-S (d-f)

Results of quantification of pore sizes and porosity of sintered samples, determined by SEM analyses and the Archimedes' method, are presented in Table 1.

Table 1. Visual open porosity and mean pore size of sintered samples prepared with polystyrene beads (G-PS-S) and cellulose fibers (G-CV-S) determined by analyses of SEM macrographs and the Archimedes' method

Sample	SEM analyses		Archimedes' met.	
	G-PS-S	G-CV-S	G-PS-S	G-CV-S
Visual open porosity, %	56	6	59.44	7.72
Mean pore size, μm	340	5	/	/
Maximal pore size, μm	807	9	/	/
Minimal pore size, μm	64	2	/	/
Standard error, μm	29	1	0.75	0.02
Standard deviation	201	2	1.69	0.05

The results of the density and compressive strength tests of the sintered samples are shown in Table 2.

Table 2. Density and compressive strength of the sintered samples prepared with polystyrene beads (G-PS-S) and cellulose fibers (G-CV-S)

Sample	G-PS-S	G-CV-S
Mean compressive strength, MPa	1.42	1.56
Standard deviation	0.032	0.022
Mean density, kg m ⁻³	1580	2210
Standard deviation	71.64	70.77

4. DISCUSSION

XRPD analyses (Fig. 1) of the green sample G-PS-G has shown that the sample contained kaolin and quartz, while peaks at the $2\theta = 9.5$ and 19° could be attributed to polystyrene [24]. After sintering, these peaks completely disappeared, which indicates that polystyrene is not present in the system anymore, which is consistent with FTIR, TGA and elemental CHNS analyses. In the green sample G-CV-G, the main phases are also kaolin and quartz while the peaks at about $2\theta = 16$ and 22° can be attributed to the presence of cellulose. As in the case of PS, these peaks disappear after sintering, which is in accordance with other reported analyses [25]. In both sintered samples, a decrease in the intensity of peaks originating from kaolinite is observed, which is a consequence of the formation of the aluminum-silicon spinel phase ($2\theta = 27$ and 40°), which transforms into mullite at higher temperatures [26].

Figure 2 shows FTIR spectra of green (G-PS-G) and sintered samples (G-PS-S) prepared with polystyrene beads. The bands at 3693 and 3619 cm⁻¹ present in the IR spectrum of G-PS-G are related to the vibration of hydroxyl groups in kaolin, *i.e.* Si—O(H)—Al, indicating the presence of these groups before sintering. Such conclusion is corroborated with the band at 1601 cm⁻¹ which is assigned to the OH bending vibration. The peaks at 2978 , 2958 and 2832 cm⁻¹ are attributed to asymmetric and symmetric stretching vibrations of the methylene group present in the PS structure. The band at 1432 cm⁻¹ is attributed to bending vibration of the C-H group [24].

The shoulders at 999 and 909 cm⁻¹ were assigned to the kaolin in-plane asymmetric Si—O—Si stretching vibration [27]. Bands at 691 and 521 cm⁻¹, which relate to symmetrical and asymmetrical Si—O—Si bending vibrations, respectively, describe the main vibration modes of the SiO₄ structure. The band pattern with peaks at 790 , 776 and 741 cm⁻¹ correspond to Al—O—Al and Al—OH structure from Al₂O₃ overlapped with symmetrical Si—O vibration [28]. Also, in this region noticeable absorption from the PS structure, *i.e.* out-of-plane deformation vibration, was observed.

Disappearance of the bands related to polystyrene and hydroxyl group in the sintered sample indicates that the PS structure decomposes after treatment at high temperatures without residual carbonaceous material in the structure of G-PS-S. After thermal treatment of G-PS-G appearance of the peak at 1034 cm⁻¹ is a result of kaolin crystallization and sintering. Also, the bands at 796 and 777 cm⁻¹ are attributed to bonds in the quartz structure, which is in accordance with results of the XRPD analysis showing a decrease in the intensity of the peaks which belong to kaolinite [29].

Green and sintered samples prepared in the presence of cellulose fibers were also studied by using FTIR spectroscopy (Fig. 3). Similar FTIR spectra of G-CV-G and G-PS-G were obtained with exception of the peak at 3327 cm⁻¹ which appears due to OH stretching vibration originating from cellulose. Small band at about 2930 cm⁻¹ is attributed to the CH stretching vibration of hydrocarbon group in cellulose. A band at 1633 cm⁻¹ is associated with the bending vibration of hydroxyl groups in cellulose and hydroxyl group at the kaolinite surface, whereas the band at 1428 cm⁻¹ is attributed to the bending vibration of C-H group [30,31]. Vibrations at wave numbers between 500 and 650 cm⁻¹ are attributed to bonds in the aluminosilicate lattice of kaolin. High similarity of the spectra of G-PS-S and G-CV-S indicate similar surface functionalities and structures of both samples, which is also confirmed by the XRPD analysis. Thermogravimetric analysis (Fig. 4) confirmed that during sintering almost all amounts of polystyrene and cellulose leave the system. Presence of insignificant amounts of organic components in the sintered samples was also examined by the CHNS analysis confirming the same results obtained by the TG analysis (*i.e.* carbon content of 0.13 and 0.1 wt.% in G-PS-S and G-CV-S, respectively).

Specific surface areas of G-PS-S and G-CV-S samples determined by the BET analysis were low amounting to $0.33 \text{ m}^2 \text{ g}^{-1}$ for G-PS-S and less than $0.2 \text{ m}^2 \text{ g}^{-1}$ for G-CV-S. A small value of specific surface area of sintered kaolin-based samples it was expected [26] and is the result of the applied sintering temperature-time regime.

SEM analysis of the sample G-PS-S (Fig. 5a-c) clearly indicates the presence of particles of different sizes, having spherical shape and spongy structure. Unlike in the case of irregularly shaped particles, the spherical particle shape ensures their proper packaging during the sintering process, which is finally manifested by obtaining the final product with the required controlled porosity. Also, rough morphology of the particle surface is noticeable. The spongy structure and rough surface morphology are the result of polystyrene decomposition. Also, SEM analysis of these samples indicates that contacts were formed between individual particles. However, in some regions increase in the contact area was not observed, so that the sintering process was not complete. In accordance with the results SEM analysis, further research should be focused on optimizing the temperature-time regime of sintering.

The sample prepared with cellulose fibers (Fig. 5d-f) did not have satisfactory porosity. The pores are rare and small in diameter, which leads to the conclusion that a much higher content of cellulose fibers in the starting ceramic paste is required to obtain open porosity, while still it is uncertain if hierarchical porosity can be obtained with this material.

As presented in Table 1, the sample G-PS-S had satisfactory visual porosity of 56 %, obtained by using only 27 wt.% of polystyrene beads. The mean pore size was $340 \mu\text{m}$. On the other hand, 30 wt.% of cellulose fibers provided visual porosity of only 6 % with the mean pore size of only $5 \mu\text{m}$. It is obvious that the lower content of polystyrene provides significantly higher porosity.

Having in mind the SEM micrographs (Figure 3 a-c), in which particles of a regular geometric shape (spheres) are clearly visible, it could be assumed that during sintering irregularities in the particle packaging did not occur resulting in a uniform pore distribution, which significantly contributed to obtaining satisfactory mechanical properties [32, 33].

Namely, density of the sample prepared with polystyrene beads was 1580 kg m^{-3} while the compressive strength reached 1.42 MPa (Table 2), which is consistent with previous research results [29]. Silicon carbide particle reinforced mullite composite foams intended for various purposes had compressive strength of 1.11 MPa at the foam density of 440 kg m^{-3} [29]. Alumina foams that were synthesized for use in photocatalytic water purification had compressive strength of 0.59 MPa [33].

The obtained results show that higher, controlled porosity and satisfactory mechanical properties are achieved when polystyrene beads are used in the synthesis instead of cellulose fibers.

5. CONCLUSION

The goal of the present research was to investigate possibilities for synthesis novel sorbents and catalyst carriers based on ceramics with controlled open porosity. Two different sacrificial templates were mixed into starting ceramic pastes to obtain open porosity: polystyrene beads (27 wt.%) and cellulose fibers (30 wt.%). Samples were sintered at $1050 \text{ }^\circ\text{C}$ for 1 h. Analyses of the obtained ceramics have shown that considerably higher open porosity was formed by using polystyrene beads (56%) than by using cellulose fibers (6 %). Also, satisfactory mechanical properties were obtained: compressive strengths were 1.42 and 1.56 MPa for samples prepared with polystyrene beads and cellulose fibers, respectively. Based on the obtained results, it can be concluded that it is possible to synthesize ceramics with controlled open porosity in the presence of polystyrene beads. These materials can find their potential application as sorbents and carriers of catalytically active substances, which will be the subject of further research through optimization of relevant parameters in the synthesis process.

Acknowledgements: This work was supported by the Ministry of Education, Science and Technological Development of the Republic of Serbia (Contracts No. 451-03-9/2021-14/200135; 451-03-9/2021-14/200288 and 451-03-68/2022-14/200288).

REFERENCES

- [1] World Health Organization (2011) Guidelines for Drinking-water Quality, 4th edn. World Health Organization, Geneva, <http://www.who.int/guidelines/en/>. Accessed June 15, 2021.



- [2] Ren Y, Yan N, Wen Q, Fan Z, Wei T, Zhang M, Ma J. Graphene/ δ -MnO₂ composite as adsorbent for the removal of nickel ions from wastewater. *Chem Eng J.* 2011; 175: 1–7. <https://doi.org/10.1016/j.cej.2010.08.010>
- [3] Hadi P, Barford J, McKay G. Synergistic effect in the simultaneous removal of binary cobalt-nickel heavy metals from effluents by a novel e-waste-derived material. *Chem Eng J.* 2013; 228: 140–146. <https://doi.org/10.1016/j.cej.2013.04.086>
- [4] Popović A, Rusmirović J, Radovanović Ž, Milošević M. Novel method of optimized synthesis of an efficient adsorbent based on vinyl modified lignin for cadmium (II) removal. In: *Processing '19, Society for Process Engineering within SMEITS*. Belgrade, Serbia, 2019, pp. 195–201
- [5] Nikolić V, Kamberović Ž, Ranitović M, Gavrilovski M, Anđić Z. Synthesis of novel WO₃/ZrSiO₄ catalysts for dehalogenation of halogenated hydrocarbons. *Metall Mater Eng.* 2019; 25: 31–37. <https://doi.org/10.30544/411>
- [6] Lindon D. Montreal Protocol on Substances that Deplete the Ozone Layer, Volume 3 B, Report of the Task Force on Destruction Technologies. <https://ozone.unep.org/treaties/montreal-protocol>, Accessed June 15, 2021.
- [7] Pawnuik M, Grzelka A, Miller U, Sówka I. Prevention and Reduction of Odour Nuisance in Waste Management in the Context of the Current Legal and Technological Solutions. *J Ecol Eng.* 2020; 21: 34–41. <https://doi.org/10.12911/22998993/125455>
- [8] Cao J, Rambo CR, Sieber H. Preparation of Porous Al₂O₃-Ceramics by Biotemplating of Wood. *J Porous Mater.* 2004; 11: 163–172. <https://doi.org/10.1023/B:JOPO.0000038012.58705.c9>
- [9] Twigg MV, Richardson JT. Theory and applications of ceramic foam catalysts. *Chem Eng Res Des.* 2002; 80: 183–189. [https://doi.org/10.1016/S0263-8762\(02\)72166-7](https://doi.org/10.1016/S0263-8762(02)72166-7)
- [10] Damoah LN, Zhang L. AlF₃ reactive Al₂O₃ foam filter for the removal of dissolved impurities from molten aluminum: Preliminary results. *Acta Mater.* 2011; 59: 896–913. <https://doi.org/10.1016/j.actamat.2010.09.064>
- [11] Sokić M, Kamberović Ž, Nikolić V, Marković B, Korać M, Anđić Z, Gavrilovski M. Kinetics of NiO and NiCl₂ hydrogen reduction as precursors and properties of produced Ni/Al₂O₃ and Ni-Pd/Al₂O₃ catalysts, *Sci World J.* 2015; 2015: 1–9. <https://doi.org/10.1155/2015/601970>
- [12] Draž A, Tomić NZ, Veličić Z, Marinković AD, Radovanović Ž, Veličković Z, Jančić-Heinemann R. Highly ordered macroporous γ -alumina prepared by a modified sol-gel method with a PMMA microsphere template for enhanced Pb²⁺, Ni²⁺ and Cd²⁺ removal. *Ceram Int.* 2017; 43: 13817–13827. <https://doi.org/10.1016/j.ceramint.2017.07.102>
- [13] Nikolić V, Kamberović Ž, Korać M, Anđić Z, Mihajlović A, Uljarević J. Nickel-based catalysts: Dependence of properties on nickel loading and modification with palladium. *Hem Ind.* 2016; 70: 137–142. <https://doi.org/10.2298/HEMIND140928090N>
- [14] Nor MAAM, Akil HM, Ahmad ZA. The effect of polymeric template density and solid loading on the properties of ceramic foam. *Sci Sinter.* 2009; 41: 319–327. <https://doi.org/10.2298/SOS0903319N>
- [15] Niesz K, Yang P, Somorjai GA. Sol-gel synthesis of ordered mesoporous alumina. *Chem Commun.* 2005; 1986–1987. <https://doi.org/10.1039/b419249d>
- [16] Deng ZY, Fukasawa T, Ando M, Zhang GJ, Ohji T. Microstructure and Mechanical Properties of Porous Alumina Ceramics Fabricated by the Decomposition of Aluminum Hydroxide. *J Am Ceram Soc.* 2001; 84: 2638–2644. <https://doi.org/10.1111/j.1151-2916.2001.tb01065.x>
- [17] de Faria CLL, de Oliveira TKR, dos Santos VL, Rosa CA, Ardisson JD, de Almeida Macêdo WA, Santos A. Usage of the sol-gel process on the fabrication of macroporous adsorbent activated-gamma alumina spheres, *Microporous Mesoporous Mater.* 2009; 120: 228–238. <https://doi.org/10.1016/j.micromeso.2008.11.008>
- [18] Nikolić V, Kamberović Ž, Anđić Z, Korać M, Sokić M. Synthesis of α -Al₂O₃ based foams with improved properties as catalyst carriers. *Materiali in Tehnologije*, 2014; 48: 45–50. http://mit.imt.si/izvodi/mit141/nikolic_v.pdf
- [19] Binner J, *Ceramic foams, Cellular ceramics: Structure, Manufacturing, Properties and Applications*. WILEY-VCH Verlag GmbH & Co. KGaA, Weinheim; 2005.
- [20] Bento AC, Kubaski ET, Sequinel T, Pianaro SA, Varela JA, Tebcherani SM. Glass foam of macroporosity using glass waste and sodium hydroxide as the foaming agent. *Ceram Int.* 2013; 39: 2423–2430. <https://doi.org/10.1016/j.ceramint.2012.09.002>
- [21] da Silva RC, Kubaski ET, Tenório-Neto ET, Lima-Tenório MK, Tebcherani SM. Foam glass using sodium hydroxide as foaming agent: Study on the reaction mechanism in soda-lime glass matrix. *Journal Non-Cryst. Solids*, 2019; 511: 177–182. <https://doi.org/10.1016/j.jnoncrsol.2019.02.003>
- [22] da Silva RC, Kubaski ET, Tebcherani SM. Glass foams produced by glass waste, sodium hydroxide, and borax with several pore structures using factorial designs. *Int J Appl Ceram Technol.* 2019; 17: 75–83. <https://doi.org/10.1111/ijac.13210>
- [23] Yatsenko EA, Goltsman BM, Klimova LV, Yatsenko LA. Peculiarities of foam glass synthesis from natural silica-containing raw materials. *J Therm Anal Calorim.* 2020; 142: 119–127. <https://doi.org/10.1007/s10973-020-10015-3>
- [24] Wankasi D, Dikio ED. Comparative Study of Polystyrene and Polymethylmethacrylate Wastes as Adsorbents for Sorption of Pb²⁺ from Aqueous Solution. *Asian J Chem.* 2014; 24: 8295–8302. <http://dx.doi.org/10.14233/ajchem.2014.16809>
- [25] Ishak WHW, Ahmad I, Ramli S, Amin MCIM. Gamma Irradiation-Assisted Synthesis of Cellulose Nanocrystal-Reinforced Gelatin Hydrogels. *Nanomaterials.* 2018; 8: 749–762. <http://dx.doi.org/10.3390/nano8100749>
- [26] Milheiro FAC, Freire MN, Silva AGP, Holanda JNF. Densification behaviour of a red firing Brazilian kaolinitic clay. *Ceram Int.* 2005; 31: 757–763. <http://dx.doi.org/10.1016/j.ceramint.2004.08.010>
- [27] Castellano M, Turturro A, Riani P, Montanari T, Finocchio E, Ramis G, Busca G, 2010. Bulk and surface properties of commercial kaolins, *Appl. Clay Science.* 2010; 48: 446–454. <http://dx.doi.org/10.1016/j.clay.2010.02.002>

- [28] Hlavay J, Jonas K, Elek S, Inczedy J, Characterization of the particle size and the crystallinity of certain minerals by IR spectrophotometry and other instrumental methods-II. investigations on quartz and feldspar, *Clays and Clay Minerals*. 1978; 26: 139-143. <https://doi.org/10.1346/CCMN.1978.0260209>
- [29] Deju R, Mazilu C, Stanculescu I, Tuca C, Fourier transform infrared spectroscopic characterization of thermal treated kaolin, *Rom Rep Phys*. 2020; 72: 1-11. <http://www.rpp.infim.ro/2020/AN72806.pdf>
- [30] Poletto M, Ornaghi HL, Zattera AJ. Native Cellulose: Structure, Characterization and Thermal Properties. *Mater*. 2014; 7: 6105-6119. <https://doi.org/10.3390/ma7096105>
- [31] Hospodarova V, Singovszka E, Stevulova N. Characterization of Cellulosic Fibers by FTIR Spectroscopy for Their Further Implementation to Building Materials, *AJAC*. 2019; 9: 303-310. <http://dx.doi.org/10.4236/ajac.2018.96023>
- [32] Akpinar S, Kusoglu IM, Ertugrul O, Onel K. Silicon carbide particle reinforced mullite composite foams, *Ceram Int*. 2012; 38: 6163-6169. <https://doi.org/10.1016/j.ceramint.2012.04.067>
- [33] Plesch G, Vargova M, Vogt UF, Gorbar M, Jesenak K. Zr doped anatase supported reticulated ceramic foams for photocatalytic water purification, *Mat Res Bull*. 2012; 47: 1680-1686. <https://doi.org/10.1016/j.materresbull.2012.03.057>

Ispitivanje mogućnosti sinteze inovativnih sorbenata i nosača katalizatora na bazi keramike kontrolisane otvorene poroznosti

Vesna D. Nikolić¹, Jovana M. Đokić², Željko J. Kamberović³, Aleksandar D. Marinković³, Sanja O. Jevtić³ i Zoran M. Anđić²

¹Inovacioni centar Tehnološko-metalurškog fakulteta, Beograd, Srbija

²Inovacioni centar Hemijskog fakulteta, Beograd, Srbija

³Univerzitet u Beogradu, Tehnološko-metalurški fakultet, Beograd, Srbija

(Naučni rad)

Izvod

Cilj ovog rada je ispitivanje mogućnosti sinteze porozne keramike sa kontrolisanom otvorenim poroznošću, koji se mogu koristiti kao sorbenti i nosači katalizatora. Dva organska dodatka su korišćena za dobijanje otvorene poroznosti: perle od polistirena i celulozna vlakna, pri čemu su bili pomešani sa prahom kaolinske gline i odgovarajućim količinama vode. Uzorci su sinterovani na 1050 °C tokom 1 h. Karakterizacija dobijenih proizvoda obuhvatala je rendgensku difrakciju praha, infracrvenu spektroskopiju sa Furijeovom transformacijom, skenirajuću elektronsku mikroskopiju (SEM), termogravimetrijsku (TGA) analizu i elementnu CHNS analizu. Pored toga, poroznost je ispitivana kvantifikacijom vizuelnih informacija sa SEM mikrofografija. Specifične površine su određene BET (engl. Brunauer–Emmett–Teller) metodom. Takođe, kod dobijenih uzoraka ispitane su gustina i čvrstoća na pritisak. Utvrđeno je da sinterovanjem organska komponenta u potpunosti izlazi iz sistema. Za uzorke pripremljene sa polistirenskim perlama i sa celuloznim vlaknima dobijene su zadovoljavajuće mehaničke karakteristike: čvrstoće na pritisak su bile 1,42 i 1,56 MPa, redom. Primećeno je da je značajno veća poroznost dobijena korišćenjem polistirenskih kuglica kao žrtvene faze (~56%) u odnosu na celulozna vlakna (~6%).

Ključne reči: porozna sinterovana glina; kaolin; polistiren; celulozna vlakna



